

Research Article

**Flavonoids of *Rosa roxburghii* Tratt exhibit anti-apoptosis
properties by regulating PARP-1/AIF[†]**

Ping Xu^{1,*} , Xingxia Liu², Xiwen Xiong³, Wenbo Zhang⁴, Xinhua Cai¹, Peiyong Qiu¹, Minghua Hao¹, Lijuan Wang¹, Dandan Lu⁵, Xiuhua Zhang⁴, Wancai Yang^{1*}

¹ Department of Pharmacy, Xinxiang Medical University, Xinxiang, Henan, 453003, China

² The Third Affiliated Hospital of Xinxiang Medical University, Xinxiang, Henan, 453003, China

³ Department of Forensic Medicine, Xinxiang Medical University, Xinxiang, Henan, 453003, China

⁴ Synthetic Biology Remaking Engineering and Application Laboratory, Xinxiang Medical University, Xinxiang, Henan, 453003, China

⁵ Institute of Radiation Medicine, Military Medical Sciences, Beijing, 100850, China

[†]This article has been accepted for publication and undergone full peer review but has not been through the copyediting, typesetting, pagination and proofreading process, which may lead to differences between this version and the Version of Record. Please cite this article as doi: [10.1002/jcb.26049]

Additional Supporting Information may be found in the online version of this article.

Received 15 December 2016; Revised 10 April 2017; Accepted 10 April 2017

Journal of Cellular Biochemistry

This article is protected by copyright. All rights reserved

DOI 10.1002/jcb.26049

***Corresponding author**

Ping Xu

E-mail address: 13273730271@163.com

Tel./fax: +8618240691447/+863733029879

Wancai Yang

E-mail address: yang3029106@126.com

Abstract

Radioprotection is an important approach to reduce the side-effects of radiotherapy. The radioprotective effect of the flavonoids of *Rosa roxburghii* Tratt (FRT) has been confirmed, and the mechanism has been identified as the Bcl-2/caspase-3/PARP-1 signaling pathway. In this study, we investigated the effects of FRT on the intercellular adhesion molecule (ICAM), and vascular cell adhesion protein (VCAM) in addition to apoptosis-related proteins such as Bax/Bcl-2, p-ERK/ERK, p-p53/p53, and p-p38/p38. In the present study, we focused on the effect of FRT on PARP-1/AIF. Ionizing radiation triggered the activation of PARP-1 and AIF translocation from the mitochondrion to the nucleus. The inhibition of PARP-1/AIF signaling pathway by FRT was investigated. Our results showed that the expressions of Bax/Bcl-2, p-ERK/ ERK, p-p53/p53 and p-p38/p38 were decreased after FRT treatment compared with the radiation-treated group. FRT inhibited PARP-1 activation to inhibit AIF translocation from mitochondrion to nucleus. Pretreatment with FRT diminished the comet's tail and reduced fragments in 6 Gy-irradiated thymocytes compared with the irradiated cells without FRT treatment. We conclude that FRT enhanced radioprotection at least partially by regulating PARP-1/AIF to reduce apoptosis. This article is protected by copyright. All rights reserved

Key Words: FRT, Thymus cells, apoptosis, PARP-1, AIF

Introduction

The apoptosis-inducing factor (AIF) is a novel apoptosis-related protein located in the inner mitochondrial membrane. The poly [ADP-ribose] polymerase 1 (PARP-1) is a nuclear protein with a dual function of promoting cell damage repair and increasing apoptosis, and an important upstream regulatory factor of AIF. In normal or DNA mildly damaged cells, PARP-1 helps repair the damaged DNA and maintain genome stability. When the DNA is badly damaged, PARP-1 is cleaved into two fragments with a relative molecular mass of 89 kD and 24 kD [Luo and Kraus, 2012].

It has been reported that AIF is activated by PARP-1 and subsequently released into the cytoplasm from the inner membrane of the mitochondria, followed by translocation to the nucleus [Sevrioukova, 2011]. Without PARP-1, AIF could not translocate from mitochondria to the nucleus in embryonic fibroblasts. The use of caspase inhibitor Z-VAD-FMK could not effectively reduce the toxicity of fibroblasts treated by H₂O₂. Therefore, it is believed that apoptosis mediated by AIF nuclear translocation is dependent on PARP-1, but not on the cascade reaction of caspase; thus, it is a non-caspase dependent apoptotic pathway [Yu et al., 2002]. It has been reported that AIF can directly cause chromatin aggregation and DNA fragmentation in the nucleus, resulting in cell apoptosis. In contrast, AIF siRNA intervention in radiation-damaged human colon cancer cells HCT-116 Bax^{-/-} could reduce DNA damage and increase cell survival rate significantly [Huerta et al., 2013]. Therefore, inhibiting the activation of PARP-1/AIF signaling pathway to reduce the damage of DNA is another effective approach for radiation protection.

Rosa roxburghii Tratt is a deciduous shrub native to China and known for its highly nutritional fruit. Flavonoids extracted from *Rosa roxburghii* Tratt (FRT) are reportedly effective antioxidants [Zhang et al., 2005]. Purity of FRT was 73.85 %. The main compounds of FRT were catechin (34.26 %) and quercetin (2.97 %) (supplementary Fig. 1/2/3). We recently reported that FRT acted as a radio-protector [Xu et al., 2014; Xu et al., 2012]. We have recently shown that FRT exhibited anti-apoptotic properties via Bcl-2 (Ca²⁺)/caspase-3/PARP-1 pathway [Xu et al., 2016]. Moreover, AIF is an important downstream molecule of PARP-1. In the present study, we investigated the effects of FRT on apoptosis-related proteins, with a particular focus on the effect of FRT on PARP-1/AIF. Ionizing radiation triggered PARP-1 activation to inhibit AIF translocation from mitochondrion to nucleus, and the inhibition of PARP-1/AIF by FRT was subsequently investigated.

Materials and Methods

Materials

Male KM mice (4–6 weeks old, weighing 18–22 g) were purchased from the Experimental Animal Center of Xinxiang Medical University. Animals were housed at 10 per cage with ad libitum access to water and food pellets. *Rosa roxburghii* Tratt was purchased from Ci-li Sales Center in Kaifeng (Henan, China; product batch 20150624). FRT was prepared in our laboratory in Xinxiang Medical University. Tissue Freezing Medium of Thermo Richard-Allan NEG-50 was purchased from Thermo Fisher Scientific Inc. (Waltham, MA USA). DNA Ladder kits were from Jian-cheng Biotechnology Co., Ltd, Nanjing, China. RPMI-1640 and fetal calf serum were obtained from Gibco BRL (Gaithersburg, USA). Antibodies for rabbit anti-poly (ADP-ribose) polymerase-1(PARP-1), and anti-apoptosis inducing factor (AIF) were purchased from Bo-Ao-Sen Biological Technology Co. Ltd, Beijing, China.

Secondary antibodies were goat anti-rabbit IgG-Cy3 and IgG-FITC from Bi-Yun-Tian Biotechnology Co., Ltd, shanghai, China. PARP-1 inhibitor (3-AB) were purchased from Selleck Chemicals (Houston, USA). RNAiso Plus reagent (TAKARA BIO INC.);

ReverTra Ace qPCR RT Master Mix kit (TOYOBO CO., LTD. Life Science Department OSAKA JAPAN); SYBR® Green Real-time PCR Master Mix kit (TOYOBO CO., LTD. Life Science Department OSAKA JAPAN).

Cell culture

Thymus cells were cultured in suspension in RPMI-1640 medium containing 10% fetal bovine serum, 100 U/mL penicillin, and 100 U/mL streptomycin at 37 °C in a humidified atmosphere of 5% CO₂.

Irradiation

Thymus cells were irradiated at room temperature with ⁶⁰Co γ-radiation at a dose of 6 Gy. The animals were restrained in holders and exposed to 6 Gy total-body ⁶⁰Co γ-radiation to determine PARP-1 and AIF.

Comet assay (alkaline single cell gel electrophoresis, ASCGE)

The thymus cells (1×10^6 cells) were treated with 50 or 100 µg/mL FRT, followed 2 h later by irradiation with ⁶⁰Co γ-radiation at a dose of 6 Gy. Two hours after irradiation, alkaline single cell gel electrophoresis (ASCGE) was performed under alkaline conditions. Ten microliters of the cell suspensions were mixed with 50 µL of 0.4% low melting point agarose. Mixtures were spread onto microscope slides pre-coated with 0.8% normal melting point agarose, and another 50 µL of 0.4% low melting point agarose were used to cover the surface. The slides were kept at 4 °C for 20 min to allow the agarose to solidify and were subsequently immersed in chilled

lysis buffer (2500 mM NaCl, 100 mM Na₂-EDTA, 100 mM Tris base pH10, 1% sarcosine Na, 1% Triton X-100, and 10% DMSO) for 1.5 h at 4 °C. Subsequently, the slides were transferred into a horizontal electrophoresis tank with chilled electrophoresis buffer (30 mM NaOH, 1 mM Na₂-EDTA) for 20 min to allow DNA unwinding. Electrophoresis was performed at 19 V and 100 mA at 4 °C for 20 min. After electrophoresis, the slides were placed in a neutralizing buffer (400 mM Tris-HCl, pH 7.5) at 4 °C for 15 min and stained with propidium iodide. Pictures of the comets were obtained by laser scanning confocal microscopy. A total of 100 comets were observed in each sample. For the analysis, the comet tail ratio was calculated.

DNA fragmentation assay (DNA ladder)

The thymus cells (1×10^6 cells) were treated with 50 or 100 µg/mL FRT. After 2 h, cells were irradiated with ⁶⁰Co γ-radiation at a dose of 6 Gy. At 3 h after irradiation, DNA gel electrophoresis was performed to assay DNA fragmentation. 5×10^5 cells were centrifuged (2000 rpm, 4 °C, 5 min), and washed with PBS for two times; 50 µL Lysis Buffer was added to the precipitate, mixed gently, centrifuged to get supernatant, to which 5 µL Enzyme A was added, reacting at 37 °C for 15 min. 5 µL Enzyme B solution was added to the suspension, gently mixed, incubated at 50 °C for 30 min; Next, adding 40 µL ammonium acetate and 200 µL cold ethanol to the mixture, mixing, reacting at 20 °C for 30 min; Then it was centrifuged (12000 rpm, 4 °C, 10 min) to obtain DNA precipitation, to which 10 µL TE Buffer was added after it was dried at room temperature for 10 min. 10 µL DNA sample solution and 2 µL Loading Buffer mixed together for electrophoresis experiment with the following conditions of 1.5% agarose gel electrophoresis and voltage 4 V/cm.

Immunoblot analysis

The thymus cells (1×10^6 cells) were treated with 50 or 100 $\mu\text{g}/\text{mL}$ FRT. After 24 h, cells were irradiated with ^{60}Co γ -radiation at a dose of 6 Gy. The PARP-1 inhibitor 3-aminobenzamide (3-AB) was added 2 h before radiation. The caspase-3 inhibitor Z-VAD-FMK was added 30 min before radiation. Six hours after irradiation, cells were collected and RIPA lysis buffer and 1 mM phenyl methyl sulfonyl fluoride (PMSF) (99:1) were added according to the amount of cells. The mixed liquid induced complete lysis and was subsequently centrifuged (4 $^{\circ}\text{C}$, 12000 r/min, 5 min). The resulting supernatant was preserved at -80 $^{\circ}\text{C}$. Forty-eight hours after transfection with PARP-1 siRNA (0.1 μM), the protein was extracted. The protein concentration was determined using the bicinchoninic acid assay (BCA) assay. The blocked blots were incubated with primary antibodies overnight at 4 $^{\circ}\text{C}$ using antibody dilutions recommended by the manufacturer. Subsequent incubation was performed with horseradish peroxidase (HRP)-conjugated secondary antibody. The signal was detected using enhanced chemiluminescence (ECL) reagents.

Detection of AIF by immunofluorescence and laser scanning confocal microscopy

Mice adapted to the environment were divided into three groups: normal (non-irradiated, untreated), irradiation (irradiated, untreated), and drug treatment (irradiated, treated). All drugs were administered orally. Mice in the normal and irradiation groups were given distilled water, and mice in the treatment groups received FRT at 30 or 60 mg/kg. After 4 d, mice were irradiated with ^{60}Co at a dose of

6 Gy. The thymuses were dissected 3 days after irradiation and were stored in 4% paraformaldehyde at 4 °C for 24 h. Fixed thymuses were put into 20% and 30% sucrose solution to be dehydrated in turn. Subsequently, the thymuses were embedded using a frozen embedding agent and were sliced into 4- μ m thick sections in Thermo Richard-Allan NEG-50. Permeabilization was performed by treating the thymic tissue sections with 0.1% Triton for 20 min. After rinsing with 0.01 M PBS for three times (5 min each), sections were incubated for 1 h in 10% normal goat serum. Tissue sections were incubated with AIF primary antibody overnight at 4 °C using antibody dilutions recommended by the manufacturer, followed by incubation with FITC-conjugated secondary antibody. Subsequently, sections were incubated for 10 min at 25 °C in 4',6-diamidino-2-phenylindole (DAPI) solution. The anti-fluorescence quenching agent was added to tissue sections in the dark. The signal was detected by laser scanning confocal microscopy.

Quantitative real-time PCR (RT-PCR)

The RT-PCR was performed according to the kit instruction. After isolating total cellular RNA using the RNAiso Plus reagent, the cDNA was acquired from 1 μ g RNA of each sample using the ReverTra Ace qPCR RT Master Mix kit according to the manufacturer's instructions as follows: 37°C for 15min, 50°C for 5min, 98°C for 5min. Quantitative PCR was performed using the ABI5500 RT-PCR system (Strata-gene) with the SYBR® Green Real-time PCR Master Mix kit with the following conditions: 95 °C for 1 min, 40 cycles of 95 °C for 15 s, 60 °C for 30 s, 72 °C for 45 s. The following primers with the predicted size were used. Primer sequence of various genes were designed as follows: **PARP-1** forward Primer: 5'-AGGACGCTGTTGAGCACTTC-3' and reverse Primer: 5'-GCTTCTTTACTGCCTCTTCG-3'; **AIF** forward Primer:

5'-CAGCCAGACAGCATCATCCA-3' and Reverse Primer:
5'-TAAAGCCGCCCATAGAAACC-3'; **GAPDH-1** forward Prime: 5'-AGGTCGG
TGTGAACGGATTTG-3' and reverse Prime: 5'-TGTAGACCATGTAGTTGAG
GTCA-3'.

Results

Effects of FRT on apoptosis-related proteins

Apoptosis signals were activated via the Bcl-2(Ca^{2+})/caspase-3/PARP-1 pathway in irradiated cells, while FRT inhibited this pathway by down-regulating cleaved caspase-3, -8, -9, and Ca^{2+} and up-regulating prototype PARP-1 and Bcl-2 [8]. As shown in Fig. 1A–E, the protein expressions of Bax, p-ERK, p-p53, p-p38 were up-regulated, while Bcl-2 was down-regulated after radiation. The ratios of Bax/Bcl-2, p-ERK/ERK, p-p53/p53, p-p38/p38 were improved. Moreover, treatment with 50 or 100 $\mu\text{g}/\text{mL}$ FRT resulted in a down-regulation of Bax/Bcl-2, p-ERK/ERK, p-p53/p53, p-p38/p38.

FRT inhibited radiation-induced cytoplasm-to-nucleus translocation of AIF *in vivo*

Given that AIF was located in mitochondria in the normal group, irradiation damage resulted in its transfer from mitochondria to nucleus. On the 1st day after irradiation, there was no apparent AIF translocation from the cytoplasm to the nucleus (Fig.2A). On the 3rd day after irradiation, the expression of protein AIF in the nucleus in thymus tissue of mice treated with irradiation but not with FRT was significantly higher compared with the normal group (Fig. 2B). On the 6th day after irradiation, no AIF was detected (Fig. 2C). Therefore, we selected 3 days after radiation as the best time to determine target molecules. Applying FRT before irradiation at the concentration of 60

mg/kg significantly inhibited AIF translocation from the cytoplasm to the nucleus (Fig. 2D).

FRT partially mitigated the radiation damage via the caspase-independent pathway of PARP-1/AIF in thymus cells

Radiation induced activation of PARP-1. Following irradiation *in vitro*, the expression of PARP-1 showed a dynamic change, which was most significant at 6 h after irradiation (Fig. 3A).

FRT inhibited the shear activation of PARP-1, without altering its integrity. As shown in Fig. 3B, the expression of PARP-1 was higher in the *FRT + PARP-1 siRNA* group than in the *PARP-1 siRNA* group. This suggests that FRT could protect PARP-1 and thus reduce degradation.

Radiation caused mitochondria to release a large amount of AIF into the cytoplasm, which was then transferred into the nucleus. As shown in Fig. 4A, the expression of protein AIF in thymus treated with irradiation was significantly higher compared with the levels in the normal group, while it was significantly lower in FRT-treated cells compared with the radiation group. Our findings suggest that the expression of AIF was significantly increased in the nucleus, and that FRT could effectively reduce its expression in the nucleus. As shown in Fig. 4B, Z-VAD-FMK has no inhibitory effect on AIF nuclear translocation. The addition of this caspase inhibitor could not prevent a large amount of AIF release caused by radiation damage. Moreover, FRT also reduced the release of AIF to reduce the radiation damage. These data indicate that FRT protected cells from radiation damage by means of a caspase-independent pathway. On

the other hand, the PARP-1 inhibitor 3-AB exerted an inhibitory effect on AIF release. As shown in Fig. 4C, after the addition of 3-AB, the release of AIF was inhibited, and there was no significant difference in the expression of AIF between the three experimental groups.

FRT protected DNA against radiation damage

Irradiation can cause different forms of DNA damage. Double-stranded breaks are one form that leads to cell death. DNA double-stranded breaks in thymocytes were examined (Fig. 5A). Irradiation induced DNA damage as evidenced by a longer comet's tail. Moreover, pretreatment with FRT diminished the comet's tail in 6 Gy-irradiated thymocytes compared with the irradiated cells without FRT treatment. The results of the DNA fragmentation assay are shown in Fig. 5B. The DNA Ladder results indicated that irradiation created more DNA fragmentation, while pretreatment with FRT reduced fragmentation in 6 Gy-irradiated thymocytes compared with only irradiated cells. Inhibitors of PARP-1 and caspase-3 administered with FRT significantly suppressed DNA fragmentation.

The effect of FRT on mRNA of AIF and PARP-1

Results on the radiation-induced activation of PARP-1 mRNA are shown in Fig. 6A. After irradiation, the expression of PARP-1 mRNA in thymocytes treated with irradiation was significantly higher compared with the levels in the normal group; while it was significantly decreased in FRT-treated cells compared with the radiation group. Radiation induced activation of AIF mRNA is shown in Fig. 6B. After irradiation, the expression of PARP-1 mRNA in thymocytes treated with irradiation

was significantly higher compared with the levels in the normal group; while it was significantly decreased in FRT-treated cells compared with the radiation group.

Discussion

Radiation often causes severe interference in the patients' quality of life, and can result in the discontinuation of the treatment due to radiation injury [Bernier, 2009; Henriquez-Hernandez et al., 2012; Ospina et al., 2015].

Exposure of cells to ionizing radiation leads to simultaneous activation of multiple signaling pathways that control cell death or survival. The molecular mechanism involved in this process has been widely explored, but not precisely deciphered [Burdelya et al., 2008; Gupta et al., 2004]. Apoptosis, or programmed cell death, is an important biological phenomenon that provides protection in response to injury whereby it minimizes further injury-related damage [Ballardin et al., 2011]. A study on gene expression in intestinal cells reported a marked increase in the Bax/Bcl-2 ratio in mice exposed to whole-body 4-Gy γ -radiation, while administration of *Clerodendron infortunatum* extract resulted in a significant reduction of this ratio, suggesting a mitigation of radiation-induced apoptosis [Chacko et al., 2016]. The radiation-induced bystander effect was diminished when the irradiated liver hepatocellular HepG2 cells were pretreated with p53 siRNA, suggesting that α -particle-induced bystander effect was regulated by p53 [Li et al., 2013]. Moreover, naringin, a major flavonoid glycoside in grapefruits, protected against ultraviolet B-induced skin damage by suppressing the mitogen-activated protein kinase (MAPK)/p38 pathway activation [Ren et al., 2016]. Following α -particle irradiation, both ERK and p38 pathways were activated in

human bronchial epithelial BEAS-2B cells, resulting in direct radiation-related damage[Fu et al., 2016]. The persistently elevated density of ICAM-1 and VCAM-1 on lung and heart microvascular endothelial cells may suggest a late inflammatory response to 8-Gy irradiation in these cells [Sievert et al., 2015].

Apoptosis is characterized by a number of cytological alterations including chromatin condensation, DNA fragmentation, and activation of cysteinyl aspartate-specific proteinases, i.e. caspases [Nicholson and Thornberry, 1997]. The pathways leading to apoptosis may be dependent or independent of caspases. Originally, caspase-dependent apoptosis was described and studied, but caspase-independent apoptosis is now a widely recognized phenomenon [Mathiasen and Jäättelä, 2002].

Recent evidence suggested AIF as an essential mediator in caspase-independent cell death [Delavallee et al., 2011]. As a highly conserved mitochondrial intermembrane flavoprotein, the mature AIF (62 kD) performs an indispensable protective redox function when anchored to the inner mitochondrial membrane [El Ghouzzi et al., 2007]. Under the stress of several pro-apoptotic signals, the mature AIF is cleaved into a soluble 57 kD protein (truncated AIF, tAIF), and exerts a special activity in inducing programmed cell death. Once released from mitochondria, AIF relocates into the nucleus and induces caspase-independent chromatinolysis, eventually leading to cell death [Cande et al., 2004]. AIF is the first identified protein involved in the caspase-independent pathway[Susin et al., 1999]. In the present study, ionizing radiation resulted in an increased expression of AIF in thymocytes and induced

mitochondrion-to-nucleus AIF translocation.

The question remains as to what is upstream of AIF. AIF was released from mitochondria by activated caspases, suggesting an involvement of caspase activation in AIF nuclear translocation [Zamzami et al., 2000]. In addition, the caspase inhibitor Z-VAD-FMK could block AIF release [Arnoult et al., 2003; Arnoult et al., 2002]. Furthermore, the translocation of the worm AIF homolog (WAH-1) translocation has been reported to require the caspase homolog cell-death gene CED-3 [Wang et al., 2002]. Taken together, these previous findings suggested that, under certain conditions, AIF release depends upon caspase activation. Our present results found that the caspase inhibitor Z-VAD-FMK failed to prevent AIF translocation, suggesting that caspase activation is not required for AIF release, at least in ionizing-radiation induced apoptosis in thymocytes.

Given that caspase was not required for the release of AIF in our experimental settings, we further investigated the factors involved in promoting AIF release. PARP-1 is activated by DNA strand breaks, which, if extensive, can initiate an energy-consuming futile intracellular cycle. This subsequently leads to rapid depletion of cellular content of NAD⁺ and ATP, which results in cell dysfunction and/or cell death [Ha and Snyder, 2000]. Cell-based studies demonstrated that diverse apoptotic stimuli including oxidative stress with concomitant energy depletion, serum deprivation, and alkylating agents cause a caspase-mediated cleavage of PARP-1; thereby allowing the cell to preserve ATP levels required for energy-dependent apoptosis and to release the suppression of apoptosis by poly(ADP-ribosyl)ated

histone H1 [Yoon et al., 1996]. Additionally, *in vivo* studies showed that inactivation of the PARP-1 gene in mice leads to pronounced protection in cerebral and myocardial ischemia-reperfusion injuries [Endres et al., 1997; Pieper et al., 2000]. Reports suggested that PARP-1, a nuclear enzyme responsible for DNA damage repairing, is an essential up-regulator of AIF translocation [Wu et al., 2012]. Over-expression of PARP-1 triggered by severe impairment could induce AIF translocation, while blocking PARP-1 could suppress translocation [Chiu et al., 2012]. Activation of nuclear PARP-1 is required for the release of AIF to the nucleus [Sevrioukova, 2011]. Moreover, the application of the PARP-1 inhibitor 3-AB inhibited the release of AIF, indicating that PARP-1 is upstream of AIF. The substantial cytoplasmic-to-nuclear translocation of AIF and its 57-kDa activated fragment detected between 14 and 24 h after treatment indicated AIF as an effector for DNA fragmentation [Meggyeshazi et al., 2014].

In summary, our findings demonstrated that PARP-1/AIF is involved in the caspase-independent cellular apoptosis induced by irradiation in thymus cells. The present research provides for the first time a potential mechanism for the application of combined ionizing radiation and gene therapy against PARP-1/AIF (Fig. 7).

Conflict of interest

The authors declare that they have no competing interests

Acknowledgments

This work was supported by the National Science Foundation of China (U1504824), Department of Science and Technology Research Project of Henan Province in China (142102310302) and the Young Teachers Plan of Higher Schools in Henan Province

(2014GGJS-098).

References

- Arnoult D, Karbowski M, Youle RJ. 2003. Caspase inhibition prevents the mitochondrial release of apoptosis-inducing factor, *Cell Death Differ* 10: 845-9.
- Arnoult D, Parone P, Martinou JC, Antonsson B, Estaquier J, Ameisen JC. 2002. Mitochondrial release of apoptosis-inducing factor occurs downstream of cytochrome c release in response to several proapoptotic stimuli. *J Cell Biol* 159: 923-29.
- Ballardin M, Tusa I, Fontana N, Monorchio A, Pelletti C, Rogovich A, Barale R, Scarpato R. 2011. Non-thermal effects of 2.45 GHz microwaves on spindle assembly, mitotic cells and viability of Chinese hamster V-79 cells. *Mutat Res* 716: 1-9.
- Bernier J. 2009. Current state-of-the-art for concurrent chemoradiation. *Semin Radiat Oncol* 19: 3-10.
- Burdelya LG, Krivokrysenko VI, Tallant TC, Strom E, Gleiberman AS, Gupta D, Kurnasov OV, Fort FL, Osterman AL, Didonato JA, Feinstein E, Gudkov AV. 2008. An agonist of toll-like receptor 5 has radioprotective activity in mouse and primate models. *Science* 320: 226-30.
- Candé C, Vahsen N, Kouranti I, Schmitt E, Daugas E, Spahr C, Luban J, Kroemer RT, Giordanetto F, Garrido C, Penninger JM, Kroemer G. 2004. AIF and cyclophilin A cooperate in apoptosis-associated chromatinolysis. *Oncogene* 23: 1514-21.
- Chacko T, Menon A, Majeed T, Nair SV, John NS, Nair CK. 2016. Mitigation of whole-body gamma radiation-induced damages by *Clerodendron infortunatum* in mammalian organisms. *J Radiat Res* 27864506.
- Chiu SC, Huang SY, Tsai YC, Chen SP, Pang CY, Lien CF, Lin YJ, Yang KT. 2012. Poly (ADP-ribose) polymerase plays an important role in intermittent hypoxia-induced cell death in rat cerebellar granule cells. *J Biomed Sci* 19:29.
- Delavallee L, Cabon L, Galan-Malo P, Lorenzo HK, Susin SA. 2011. AIF-mediated caspase-independent necroptosis: a new chance for targeted therapeutics. *IUBMB Life* 63: 221-32.
- El Ghouzzi V, Csaba Z, Olivier P, Lelouvier B, Schwendimann L, Dournaud P, Verney C, Rustin P, Gressens P. 2007. Apoptosis-inducing factor deficiency induces early mitochondrial degeneration in brain followed by progressive multifocal neuropathology. *J Neuropathol Exp Neurol* 66: 838-47.
- Endres M, Wang ZQ, Namura S, Waeber C, Moskowitz MA. 1997. Ischemic brain injury is mediated by the activation of poly(ADP-ribose)polymerase. *J Cereb Blood Flow Metab* 17: 1143-51.
- Fu J, Wang J, Wang X, Wang P, Xu J, Zhou C, Bai Y, Shao C. 2016. Signaling factors and pathways of α -particle irradiation induced bilateral bystander responses between Beas-2B and U937 cells. *Mutat Res* 789:1-8.
- Gupta D, Arora R, Garg AP, Bala M, Goel HC. 2004. Modification of radiation damage to mitochondrial system in vivo by *Podophyllum hexandrum*: mechanistic aspects. *Mol Cell Biochem* 266: 65-77.
- Ha HC, Snyder SH. 2000. Poly(ADP-ribose) polymerase-1 in the nervous system. *Neurobiol Dis* 7: 225-39.

- Henriquez-Hernandez LA, Bordon E, Pinar B. 2012. Prediction of normal tissue toxicity as part of the individualized treatment with radiotherapy in oncology patients. *Surg Oncol* 21: 201-6.
- Huerta S, Gao X, Dineen S, Kapur P, Saha D, Meyer J. 2013. Role of p53, Bax, p21, and DNA-PKcs in radiation sensitivity of HCT-116 cells and xenografts. *Surgery* 154(2):143-51.
- Li J, He M, Shen B, Yuan D, Shao C. 2013. Alpha particle-induced bystander effect is mediated by ROS via a p53-dependent SCO2 pathway in hepatoma cells. *Int J Radiat Biol* 89:1028-34.
- Luo X & Kraus WL. 2012. On PAR with PARP: cellular stress signaling through poly(ADP-ribose) and PARP-1. *Genes Dev* 26: 417-432.
- Mathiasen I, Jäättelä M. 2002. Triggering caspase-independent cell death to combat cancer. *Trends Mol Med* 8: 212-20.
- Meggyeshazi N, Andocs G, Balogh L, Balla P, Kiszner G, Teleki I, Jeney A, Krenacs T. 2014. DNA fragmentation and caspase-independent programmed cell death by modulated electrohyperthermia. *Strahlenther Onkol* 190: 815-22.
- Nicholson DW, Thornberry NA. 1997. Caspases: killer proteases. *Trends Biochem Sci* 22: 299-306.
- Ospina, JD, Fargeas A, Drean G. 2015. Recent advancements in toxicity prediction following prostate cancer radiotherapy. *Conf. Proc. IEEE Eng. Med Biol Soc* 8: 5231-34.
- Pieper AA, Walles T, Wei G, Clements EE, Verma A, Snyder SH, Zweier JL. 2000. Myocardial postischemic injury is reduced by polyADPribose polymerase-1 gene disruption. *Mol Med* 6: 271-82.
- Ren X, Shi Y, Zhao D, Xu M, Li X, Dang Y, Ye X. 2016. Naringin protects ultraviolet B-induced skin damage by regulating p38 MAPK signal pathway. *J Dermatol Sci* 82:106-14.
- Sevrioukova IF. 2011. Apoptosis-inducing factor: structure, function, and redox regulation. *Antioxid Redox Signal* 14: 2545-2579.
- Sievert W, Trott KR, Azimzadeh O, Tapio S, Zitzelsberger H, Multhoff G. 2015. Late proliferating and inflammatory effects on murine microvascular heart and lung endothelial cells after irradiation. *Radiother Oncol* 117:376-81.
- Susin SA, Lorenzo HK, Zamzami N, Marzo I, Snow BE, Brothers GM, Mangion J, Jacotot E, Costantini P, Loeffler M, Larochette N, Goodlett DR, Aebersold R, Siderovski DP, Penninger JM, Kroemer G. 1999. Molecular characterization of mitochondrial apoptosis-inducing factor, *Nature* 397: 441-6.
- Wang X 1, Yang C, Chai J, Shi Y, Xue D. 2002. Mechanisms of AIF-mediated apoptotic DNA degradation in *Caenorhabditis elegans*, *Science* 298: 1587-92.
- Wu W, Liu P, Li J. 2012. Necroptosis: an emerging form of programmed cell death. *Crit Rev Oncol Hematol* 82: 249-58.
- Xu P, Zhang WB, Cai XH, Lu DD, He XY, Qiu PY, Wu J. 2014. Flavonoids of *Rosa roxburghii* Tratt Act as Radioprotectors. *Asian Pac J Cancer Prev* 15: 8171-75.
- Xu P, Yan XQ, Chen HT. 2012. Application of flavonoids from *Rosa roxburghii* Tratt in

medicine preparation for protection against ionizing radiation. State Intellectual Property Bureau in the People's Republic of China ZL201010570876.1.

Xu P, Cai XH, Zhang WB, Li YN, Qiu PY, Lu DD. 2016. Flavonoids of *Rosa roxburghii* Tratt exhibit radioprotection and anti-apoptosis properties via the Bcl-2(Ca²⁺)/caspase-3/PARP-1 pathway. *Apoptosis* 21: 1125-43.

Yoon YS, Kim JW, Kang KW, Kim YS, Choi KH, Joe CO. 1996. Poly(ADP-ribosylation) of histone H1 correlates with internucleosomal DNA fragmentation during apoptosis. *J Biol Chem* 271: 9129-34.

Yu SW, Wang H, Poitras MF, Coombs C, Bowers WJ, Federoff HJ, Poirier GG, Dawson TM, Dawson VL. 2002. Mediation of poly (ADP-ribose)Polymerase-1 dependent cell death by apoptosis-inducing factor. *Science* 297 (5579) : 259-263

Zamzami N, El Hamel C, Maisse C, Brenner C, Muñoz-Pinedo C, Belzacq AS, Costantini P, Vieira H, Loeffler M, Molle G, Kroemer G. 2000. Bid acts on the permeability transition pore complex to induce apoptosis, *Oncogene* 19: 6342-50.

Zhang XL, Qu WJ, Sun B. 2005. In vitro antioxidant effects of flavonoids of *Rosa*. *Nat Prod Res and Dev* 17(4): 396-400.

Figure legends

Fig. 1 Effects of FRT on apoptosis related proteins as measured by Western blot.

(A) Effect of FRT on the expression of Bax/Bcl-2 in thymocytes after irradiation (*, $P < 0.01$ compared with control; #, $P < 0.01$ compared with irradiation alone). (B) Effect of FRT on the expression of p-ERK/ ERK in thymocytes after irradiation (*, $P < 0.01$ compared with control; #, $P < 0.01$ compared with irradiation alone). (C) Effect of FRT on the expression of p-p53/p53 in thymocytes after irradiation (*, $P < 0.01$ compared with controls; #, $P < 0.01$ compared with irradiation alone). (D) Effect of FRT on the expression of p-p38/p38 in thymocytes after irradiation (*, $P < 0.01$ compared with controls; #, $P < 0.01$ compared with irradiation alone). (E) Effect of FRT on the expression of ICAM and VCAM in thymocytes after irradiation (*, $P < 0.01$ compared with controls; #, $P < 0.01$ compared with irradiation alone).

Fig. 2 FRT inhibited radiation-induced translocation of AIF from cytoplasm to nucleus *in vivo*. (A) AIF at 1 d after irradiation. (B) AIF at 3 d after irradiation. (C) AIF at 6 d after irradiation. (D) Effect of FRT on the translocation of AIF from cytoplasm to nucleus *in vivo* (*, $P < 0.01$ compared with controls; #, $P < 0.01$ compared with irradiation alone).

Fig. 3 Effects of FRT on the expression of PARP-1 siRNA in thymocytes as measured by Western blot. (A) The activation of PARP-1 at different time points after irradiation (*, $P < 0.01$ compared with controls). (B) Effect of FRT on the expression of PARP-1 in thymocytes following PARP-1 siRNA transfection (*, $P < 0.01$ compared with Ps group).

Fig. 4 Effects of FRT on the expression of AIF in thymocytes after irradiation as measured by Western blot. (A) Effects of FRT on the expression of AIF in the cytoplasm and nucleus *in vitro*. (*, $P < 0.01$ compared with controls; **, $P < 0.01$ compared with irradiation alone). (B) Effect of caspase-3 inhibitor Z-VAD-FMK on the expression of AIF after irradiation (*, $P < 0.01$ compared with controls; **, $P < 0.01$ compared with irradiation alone). (C) Effect of PARP-1 inhibitor 3-AB on the expression of PARP-1 and AIF after irradiation.

Fig. 5 Protective effect of FRT on irradiation-induced DNA damage in thymocytes. (A) Effect of FRT on irradiation-induced DNA comet's tail in thymocytes. DNA damage was detected by the alkaline single-cell gel electrophoresis (ASCGE) assay. One hundred comets were analyzed in each group, and percentages of tail DNA were compared (*, $p < 0.01$ compared with controls; #, $p < 0.01$

compared with irradiation alone). (B) Protective effect of FRT on irradiation-induced DNA fragmentation in thymocytes.

Fig. 6 Effect of FRT on PARP-1/AIF mRNA in irradiated thymocytes. (A) Effect of FRT on PARP-1 mRNA in irradiated thymocytes (*, $p < 0.01$ compared with controls; #, $p < 0.01$ compared with irradiation alone). (B) Effect of FRT on AIF mRNA in irradiated thymocytes (*, $p < 0.01$ compared with controls; #, $p < 0.01$ compared with irradiation alone).

Fig. 7 PARP-1/AIF signal pathway

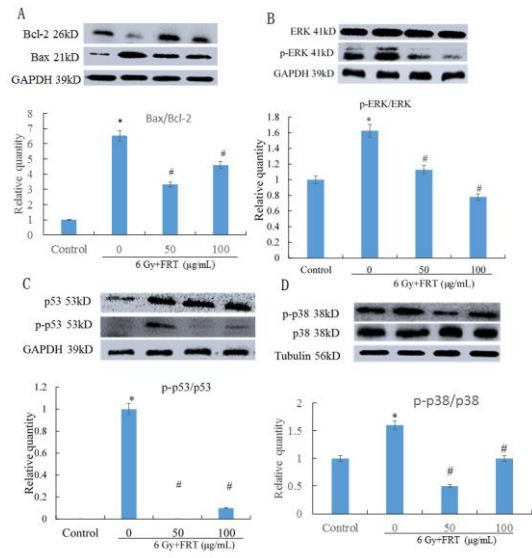


Figure 1

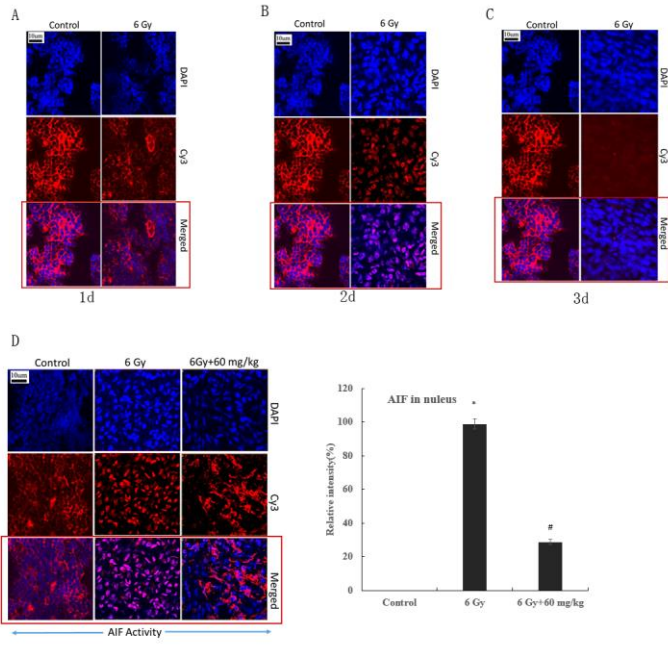


Figure 2

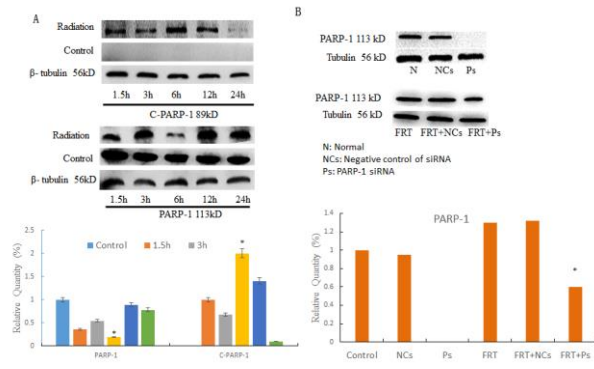


Figure 3

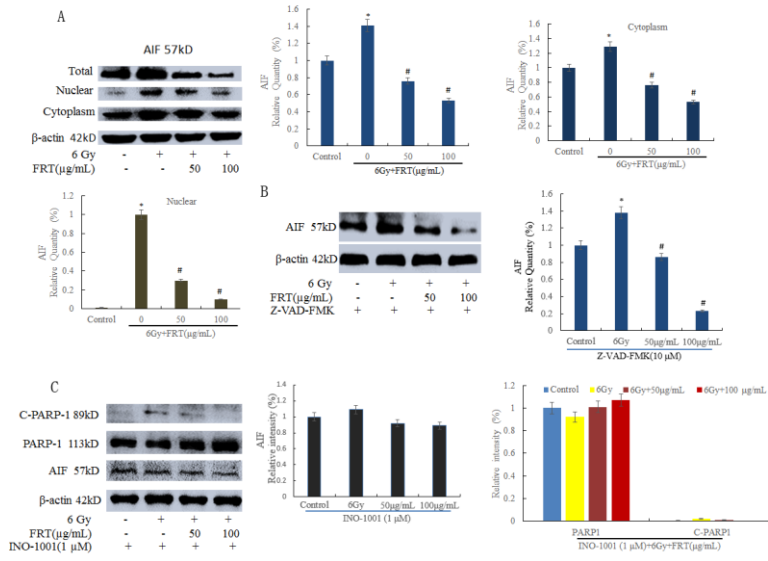


Figure 4

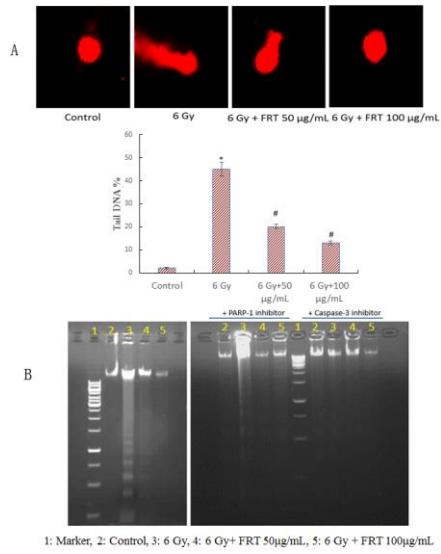


Figure 5

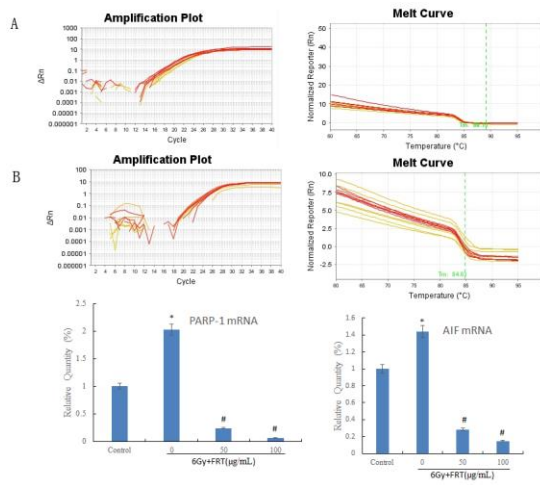


Figure 6

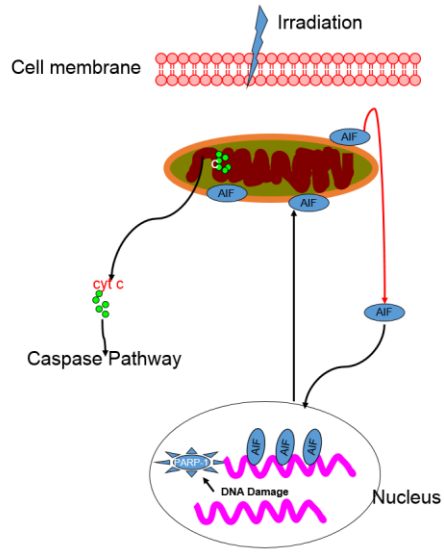


Figure 7